Journal of Solar Energy Research (JSER)

Journal homepage: jser.ut.ac.ir

An experimental study of the effect of using Ag-water nanofluid in different concentrations on the performance of circular collectors

Mojtaba Moravej[a], Fateme Namdarnia[b], Leila Partabian[b]

[a]*Department of Mechanical Engineering, Payame Noor University, Iran*
[b] *Graduated, Payame Noor University, Iran*
Received: 2021-12-31
Accepted: 2022-02-17

Abstract

The utilization of nanofluids as heat transfer fluid is an effective way to increase the efficiency of solar collectors. In this research, the performance of a circular flat-panel solar collector with spiral coolant passage projected from the periphery to the center of the circle, which is like a sunflower, has been studied experimentally according to the ASHRAE standard in Aghajari (latitude 30^0 $69^{/}$ $8^{//}$ N, longitude 49^0 $82^{/}$ $40^{//}$ E) in southern Iran. Pure water and silver-water nanofluid in three mass concentrations of 0.1%, 0.2% and 0.3% have been used for evaluating collector thermal efficiency in different conditions. The results show that compared to pure water, silver-water nanofluid has a better performance and increasing silver nanoparticles from 0.1% to 0.3% improves the collector thermal efficiency by around 5.7%. Also, the efficiency of the collector becomes higher after increasing solar irradiation. In addition, it is observed that there is no relationship between air humidity and efficiency. The highest efficiency obtained from this collector at a volume fraction of 0.3% and coolant flow rate of 2.268 lit/min was about 80.3%, which is14.8% more than that of pure water.

Keywords: Solar collector, Circular flat-plate, Silver-water nanofluid, Efficiency, Experimental test.

1. Introduction

Global concern regarding environmental footprint due to the immoderate use of fossil fuels is increasing. So, demand for exploiting the potential of renewable resources has raised significantly. The viability and desirability of solar energy as a type of alternative energy is undeniable. Among solar technologies, flat-plate solar collector due to simplicity and high effectiveness has caught a lot of attention[1, 2]. One of the important criteria for evaluating flat plate collectors is their efficiency and effectiveness, which depends on various factors such as absorber, collector geometry, pipes containing fluid, type of fluid. Utilizing water-based nanofluid is an efficient approach to enhance solar collector performance [3-6]. The work of Sakhaei [7] focused on utilizing a model of tubes in the risers to improve the flat-plate collector thermal efficiency. They performed several experiments on these collectors during the turbulence period according to ASHRAE standard and showed that the maximum efficiency

*corresponding author Email address

was approximately 61.59% at a Reynolds number of 5153.

Sundar et al. [8] conducted a comprehensive study of flat panel collectors with cylindrical torsion risers. In this study, exergy, economic analysis and efficiency of the solar system were reviewed. The results of the study indicated that the collector efficiency in the flow of 300 liters per hour is more than 37% compared to pure water when using water-alumina nanofluid with a volume fraction of 0.3%.

Nogharabadi et al. [9] used silica-water nanofluid in a symmetric solar collector and proved that the spiral tubes used in this collector have a remarkable influence on increasing the collector efficiency. Besides, the impact of increasing solar irradiance on enhancing efficiency for solar collectors filled with nanofluid was greater than that of pure water.

Moravej et al [10] used titanium dioxide-water nanofluid in a symmetrical square collector and showed that along with increasing the concentration, a significant increase in collector efficiency is achieved, especially in high solar discharges and radiation.

Rajput [11] Experimental study using water-alumina nanofluid in solar flat plate collector and showing that using this nanofluid with a volume concentration of 0.3% and a volume flow rate of 1.3lit / min increases the collector efficiency by more than 21% compared to It is purified with water.

Zayed et al. [12] presented a review study on the impact of using various nanofluids on the solar flat panel performance in different conditions. He considered the heaviest nanoparticles used to be related to silver and Lee reported the highest increase in efficiency to the two nanofluids of copper-water and alumina-water with a maximum of 37% and 31% growth in yield, respectively.

Wole-Osho et al. [13] studied the economy, exergy and energy of using hybrid nanofluid in a flat- plate solar collector. They concluded that the maximum obtained efficiency of a collector by using hybrid Al2O3-ZnO-Water nanofluid was about 66% and the exergy range was under 83%.

Stalin et al [14] conducted a comprehensive experimental study including environmental, economic and energy impacts on flat plate collectors utilizing CeO_2-water nanofluid. It was reported that the thermal efficiency of the collector was improved up to 28% by replacing pure water with CeO_2-water nanofluid. They also reported maximum exergy of 5.8% and a decrease in carbon dioxide emissions of 175 kg.

Research into using CuO nanofluid in the flat plate solar collectors hasbeen investigated experimentally by Mirzaei [15]. He found that the thermal efficiency of collectors can be enhanced up to 55.1% by using CuO nanofluid instead of pure water.

Eidan et al. [16] conducted a two-part experimental study on a solar collector using aluminum oxide nanoparticles and acetone-based copper oxide nanoparticles. He also evaluated the tilt angle of the collector in three different values. The results of the studies indicated that the selection of the optimal angle of 45 degrees and using mentioned nanoparticles can increase the efficiency between 15-38%

Kilic et al. [17] explored the effect of using titanium oxide-water on the flat plate collector performance according to the en-ISO-9806 standard and using surfactant. In the end, they reported a maximum efficiency of 48% for nanofluids and 36% for water.

In an interesting study, Okonkow [18] examined the AL2O3-FE-WATER hybrid nanofluid in comparison with the AL2O3-water nanofluid in the flat plate collector with a maximum concentration of 0.2%. It was at least 0.05%. In the end, it was found that AL2O3-water nanofluid has greater performance in increasing efficiency, while the increase in exergy was more in a hybrid nanofluid.

Yan et al. [19] used a movable cover for the flat plate collector, which was modeled based on an extended dynamic heat transfer model and compared with experiments. His analysis was based on environmental parameters and with different conditions in summer and winter. The results showed that the collector can reduce heat loss by up to 62.8%.

Nogarabadi et al. [20] experimentally analyzed a three-dimensional collector with conical geometry and spiral tubes. In this collector, the pipes containing the fluid were drawn in a spiral from the bottom to the top of the cone. In the experimental analysis, the result showed that the collector

efficiency reaches up to 60%. Sakhaei and Valipour [21] evaluated the performance of solar flat panel collectors by considering various parameters. He reviewed many previous studies and said that one of the best cases for new studies was helical turbochargers for risers with nanofluids.

According to a review of research, it has been found that the use of circular collectors and spiral tubes to increase heat transfer even with less nanofluid has been considered. In this research, a circular flat plate solar collector containing spiral tubes is projected from the edge of the circle to the center of the circle. This collector is inspired by the appearance of sunflower and is fixed and without a trace, which has been studied and tested by Ag-water nanofluid in three different concentrations and pure water according to ASHREA standard.

2. Materials and Methods

The laboratory layout and method of testing and data collection along with how the collectors are placed in the process of absorbing radiation from the sun and transferring heat to the operating fluid is presented in Fig. 1. According to this figure, it is clear that the operating fluid in the initial state (cold) after entering the collector, is heated by passing through the pipes connected to the absorber and the hot fluid leaves the collector. The collector specifications are illustrated in Table 1. To measure the test data, different measuring instruments were used, the specifications of each of which are presented in Table 2. All measuring devices were calibrated before the start of the tests and after the test at the end of the day were collected and cleaned and used again the next day. Performance evaluation of the collector was done under ASHRAE standard [22] and the conditions of this standard are shown in Table 3.

For a better and more comprehensive evaluation, both collectors are located near the university educational building in an open area. The test site was Payame Noor University of Aghajari city in southern Iran at an elevation of 131 meters above sea level, with a longitude of 30 degrees and 69 minutes north and a latitude of 49 degrees and 82 minutes east. The collector was active in the early hours of the morning to evening and the data collection was done every 15 minutes. To evaluate more accurately and eliminate inaccurate data, the time presented in the results was selected from the best data in 120 minutes after logged data. The collector performance is measured according to the ASHRAE standard and the collectors are constantly exposed to sunlight and fluid flow generated by the electric diaphragm pump, and the data are recorded in stable and quasi-stable conditions. The experiments were repeated regularly and were performed in different data collection conditions. Fig. 2 shows the actual photo of the collector setup.

Table 1. Collector specifications

Specifications	Units
Absorber area	1 m^2
Absorber thickness	1.25 mm
Piping	Copper helical pipe
Pipe external diameter	12.4 mm
Glass cover	Flat glass with 6 mm thickness
Insulation	MDF wood with 16 mm thickness

Table 2. Measurement devices

Devices	Accuracy
Solar meter	1 W/m^2
Flow meter	0.378 lit/min
Thermo meter	0.1 ^{0} C
Humidity meter	1%
Wind speed meter	0.1 m/s

Table 3. Maximum variation of important parameters [10]

Parameters	Maximum variation
Total solar irradiance normal to surface (W/m^2)	±32
Ambient temperature (K)	±1.5
Volumetric flow rate	The greater of ±2% or ±0.0013(lpm)
Inlet temperature	The greater of ±2% or 1 (K)

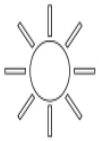

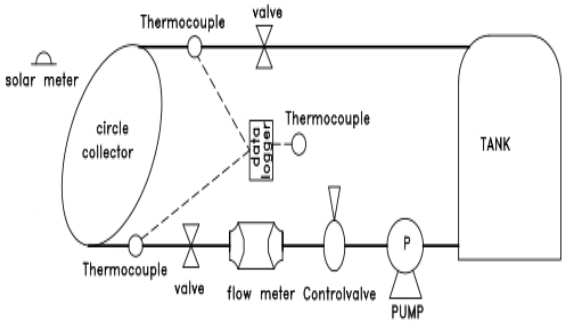

Figure 1. Setup of the experiment

Figure 2. Photo of a real test scene

2-1-Collector time constant

One of the important aspects of the solar collector performance is the calculation of heat capacity with regard to the time constant. The time constant is expressed as the time needed for the outlet temperature to have a total variation of 63% from its initial value to its final value. Time constant is formulated as Eq. (1) [23].

$$\frac{e}{T_{O,i} - T_i} = \frac{1}{T_{O,r} - T_i} \qquad (1)$$

Where T_i and $T_{O,r}$ are inlet and outlet fluid temperature respectively and $T_{O,i}$ is outlet fluid temperature when the solar irradiance is stopped.

2-2-Preparation of nanofluids

In principle, the preparation and production of nanofluids are possible in two ways, single-stage and two-stage methods. In the two-step method that has been studied in this research, first, the desired nanoparticles are prepared and then in the base fluid under special conditions of solution and suspension of nanoparticles, the fluid is obtained. For this production method, in addition to solution formation, homogenizers and ultrasonic baths are used to prepare a suspension with homogeneous distribution and properties. For this research, nanofluids from the Nanosadra-Iran company have been used. The type of silver nanoparticles is from US7150 model with an approximate size of 5-8 nm, which is produced in three concentrations of 0.1%, 0.2% and 0.3% based on ordinary water fluid. Fig. 3 shows the Intensity curve of nanoparticles, and Fig. 4 shows the nanofluid produced and used.

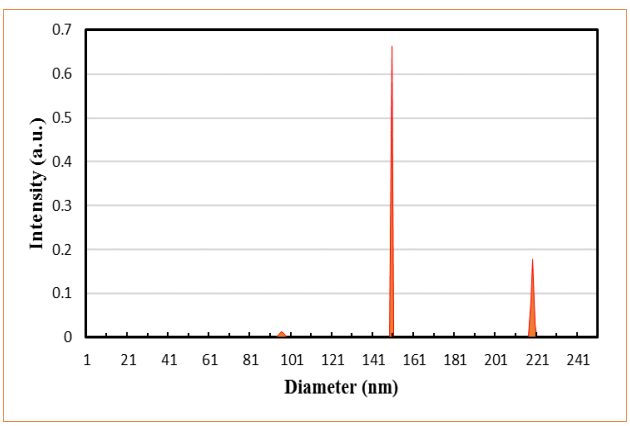

Figure 3. DLS diagram of nanoparticles used in the preparation of nanofluids

Figure 4. Nanofluid used in three concentrations

3-2-Required equations

One of the key indicators to evaluate the performance of solar collectors is their thermal efficiency which is the ratio between actual useful energy and the rate of emitted solar irradiance. The actual useful thermal energy obtained by the collector can be expresses as Eqs. (2) and (3) [4, 23].

$$Q_u = \dot{m}C_p(T_o - T_i) \quad (2)$$

By introducing F_R as collector heat removal factor, which is given in Eq. (3), the actual useful energy can be rewritten as Eq. (4) [4, 23].

$$F_R = \frac{\dot{m}C_p(T_o - T_i)}{A_c[G_T(\tau\alpha) - U_L(T_i - T_a)]} \quad (3)$$

$$Q_u = A_c[F_R G_T(\tau\alpha) - F_R U_L(T_i - T_a)] \quad (4)$$

The amount of heat transferred to the heat transfer fluid which is equal to actual useful energy is calculated based on the specific heat of the fluid. The specific heat of the fluid is obtained from Eq. (5) [7, 10].

$$C_{p,nf} = C_{p,np}(\varphi) + C_{p,bf}(1 - \varphi) \quad (5)$$

In which, $C_{p,np}$ is the heat capacity of the nanoparticle, φ is the nanoparticles concentration, and $C_{p,bf}$ is the heat capacity of a base fluid.

The efficiency of the collector can be expressed as Eq. (6) [23].

$$\eta_i = \frac{Q_u}{A_c G_T} = \frac{\dot{m}C_p(T_o - T_i)}{A_c G_T} \quad (6)$$

Based on the Eqs. (3) and (6), the efficiency of the solar collector can be rewritten as Eq. (7) [23].

$$\eta_i = F_R(\tau\alpha) - F_R U_L\left(\frac{T_i - T_a}{G_T}\right) \quad (7)$$

In the above equation, $F_R(\tau\alpha)$ and $F_R U_L$ are parameters that indicate how the solar collector operates, where $F_R(\tau\alpha)$ is representative of energy absorbed by the collector and $F_R U_L$ is representative of energy lost from collector.

3-3-Uncertainty analysis

Preforming uncertainty analysis for all parameters measured during experimental tests is crucial as certain the accuracy of results. To determine the uncertainty in the tests, the ROOT SUM SQAURE METHOD (RSSM) was utilized, which is computed from Eq. (8) [24].

Assume R is a function of some independent variable, so we have:

$$R = f(x_1, x_2, \ldots, x_n) \quad (8)$$

If R is a multiplicative function of the variables then R and its derivative will be as follows:

$$R = x_1^{a_1} x_2^{a_2} \ldots x_n^{a_n} \quad (9)$$

$$\frac{1}{R}\frac{\partial R}{\partial x_i} = \frac{a_i}{x_i} \quad (10)$$

$$\frac{\omega_R}{R} = \left[\sum_{i=1}^{n}\left(\frac{a_i \omega_{x_i}}{x_i}\right)^2\right]^{\frac{1}{2}} \quad (11)$$

Where $(\frac{\omega_R}{R})$ is the uncertainty of function (R). Also Eq. (6) can be write by following:

$$\eta = \dot{m}^1 C_p{}^1 \Delta T^1 G_T{}^{-1} A^{-1} \quad (12)$$

By using Eqs. (11&12) the result will be as bellow:

$$\frac{\omega_\eta}{\eta} = \left[\left(\frac{1\omega_{\dot{m}}}{\dot{m}}\right)^2 + \left(\frac{1\omega_{C_p}}{C_p}\right)^2 + \left(\frac{1\omega_{\Delta T}}{\Delta T}\right)^2 + \left(\frac{-1\omega_{G_T}}{G_T}\right)^2 + \left(\frac{-1\omega_A}{A}\right)^2\right]^{1/2} \quad (13)$$

According to the calculations and measurements, the amount of uncertainty calculated for the above data in Table 4 and Eq. (13), the uncertainty of calculating the efficiency of collectors $(\frac{\omega_\eta}{\eta})$ is about 6.3%.

Table 4. Uncertainty of measuring parameters

Parameter	Uncertainty (%)
Solar irradiance ($\frac{\omega_{G_T}}{G_T}$)	3.1
Temperature ($\frac{\omega_{\Delta T}}{\Delta T}$)	0.2
Area ($\frac{\omega_A}{A}$)	0.01
Volume flow rate ($\frac{\omega_{\dot{m}}}{\dot{m}}$)	5.5
Specific heat ($\frac{\omega_{C_p}}{C_p}$)	0 (constant)

3. Results and discussion

Withregard to evaluating the performance of the introduced solar collector, the pipes inside the collector were first washed several times with pure water. Then, at an angle of 45 degrees to the horizon, the collector was placed at the test site and pipes containing the working fluid are installed at the inlet and outlet according to Fig. 1. All measuring instruments were located in a suitable place and then the data is taken. The process of measuring and collecting data is such that first, the fluid flow is adjusted with the control valve and then other data such as environmental conditions and temperatures are recorded. Also, the recording time of all the above data, including temperatures and other data, in total at each stage have a time difference of less than two minutes. Experiments have been performed repeatedly and the best data have been selected and presented. This data was collected in sunny weather and almost without clouds and was evaluated and examined.

Fig. 5 shows the amount of solar irradiance arriving at the collector surface that is measured directly by a solar meter. Given that the area of the collector adsorbent surface is practically one square meter, the amount of input flux will be equal to the measured radiation. In other words, in the vertical axis of Figure 5, both W and W / m2 radiation can be displayed without any change in the data. Examination of the graph shows that the radiation starts at lower values at the beginning of the experiment and peaks around noon and then decreases.

Fig. 6 shows the wind speed in terms of m / s and relative humidity. In fact, at the same time as measuring the thermal performance and fluid temperatures in different places, the velocity and humidity of the air are also evaluated. The important point in measuring these data is that because of collecting datain the second half of the year,the relative decrease in solar radiation compared to the summer and the increase in humidity and wind speed increases heat loss while disrupting the test and exit process. Therefore, the recorded wind speed is equal to the maximum wind speed at that moment in all directions and the humidity is measured at a distance of at least two meters from the collector. According to the data obtained, the maximum wind speed in all experiments was less than 6 m / s and humidity was less than 65%.

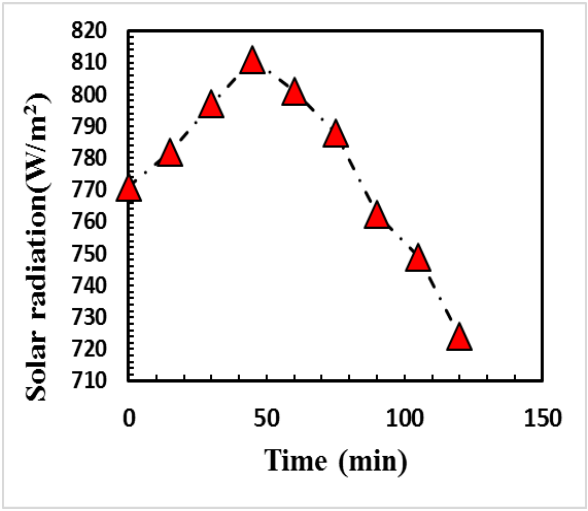

Figure 5. Diagram of the radiation reaching the collector during the test

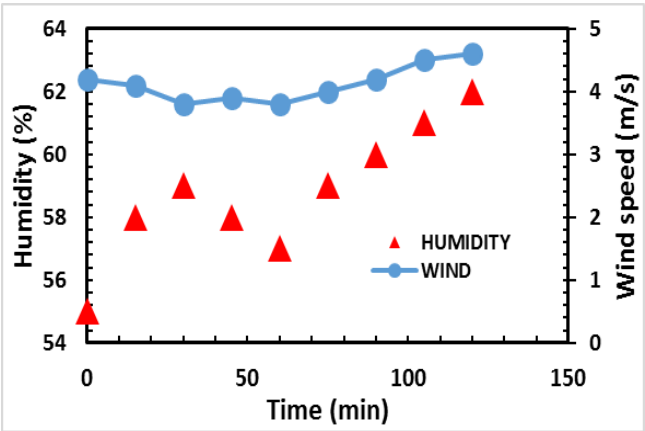

Figure 6. Measured environmental parameters; Wind speed and Humidity

Figs. 7 and 8 indicate the efficiency of the circular collector as a function of time and the temperature difference between the inlet and outlet of the heat transfer fluid as a function of incident solar irradiation for pure water and three concentrations of nanofluid. As can be seen in these two figures, with

increasing time and radiation, the amount of solar radiation also increases. Additionally, the inlet temperature of the collector also increases slightly. This is because the nanofluid that comes out of the collector and returns to the collector cycle gets a little warmer at each stage. Therefore, with increasing time, the collector efficiency increases continuously and reaches its peak during maximum irradiation, and then has a decreasing trend. It should be noted that the decreasing slope of efficiency after the peak is less than before reaching the peak due to the impact of higher temperature on the heat transferred to the operating fluid, especially when using nanofluids. Another important point is the variation of thermal efficiency with respect to nanofluid concentration and inlet-outlet temperature difference. With the increment of nanofluid concentration, the value of efficiency and temperature difference becomes higher.

Fig. 9 represents the influence of the Reynolds number on the performance of a circular collector. It is obvious that with increasing flow rate, collector efficiency increases owing to the direct role of the Reynolds number and consequently the Nusselt number. However, because of the effect of the presence of stray nanoparticles with different movements, including Brownian movements, the growth of efficiency when using nanofluids will be more than the use of pure water. It also should be noted that the higher the nanoparticle concentration, the greater the collector thermal efficiency because the heat transfer from the pipe wall to the operating fluid increases, which in turn enhances thermal efficiency.

Fig. 10 shows the collector efficiency diagrams in different fluids based on the relative humidity of the air. It can be seen that increasing the humidity causes heat loss and reduces efficiency.However, due to the range of humidity changes, which is less than 10%, the variation of efficiency in different nanofluid concentrations is insignificant. Environmental parameters such as radiation and inlet temperature to the collector will be much higher than air humidity. The important point of this diagram is that almost all concentrations of nanofluid and ordinary water behaved similarly to changes in the air humidity, which means that the effect of this parameter on collector thermal efficiency is independent of the nanofluid concentration.

Fig. 11 uses the effect of nanofluids at three different concentrations for the final summation and comparing them with the base fluid. The maximum efficiency values obtained under the same conditions are presented. The role of concentration in this diagram is clear and as the concentration increases, so does the efficiency. However, this efficiency growth is not proportional to the concentration of a linear growth and, as shown in the regression in the diagram, has a nonlinear performance derived from the effects of other parameters affecting the concentration, including secondary flow and suspended nanoparticle movements. According to Eq. (7) there is a linear relation between the collector efficiency and $\left(\frac{T_i-T_a}{G_T}\right)$ parameter. Due to having Ti, Ta, G_T and the calculated efficiency, we can find this linear relationship. On the other hand, if we draw a line between $\left(\frac{T_i-T_a}{G_T}\right)$ and η_i , we have $F_R(\tau\alpha)$ and $F_R U_L$ as maximum efficiency and line slope respectively. According to Equation (7), the efficiency diagram is linear based on the temperature decrease parameter (Ti-Ta/G_T). This diagram is presented in Fig. 12. In this diagram, the data may not exactly match the line due to a measurement error. The intersection of these lines with the vertical axis is equal to the maximum efficiency, $F_R(\tau\alpha)$, in that fluid and the slope of the graph is equal to $F_R U_L$. These values are shown in Table 5. Table 6 shows a comparison between present study and previous research.

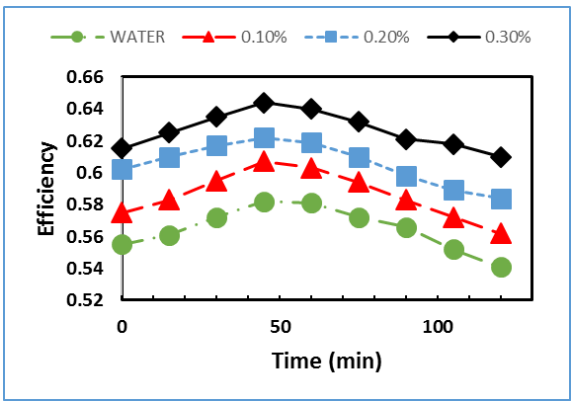

Figure 7. Comparison of the effect of nanofluid use on collector performance(Re=6004)

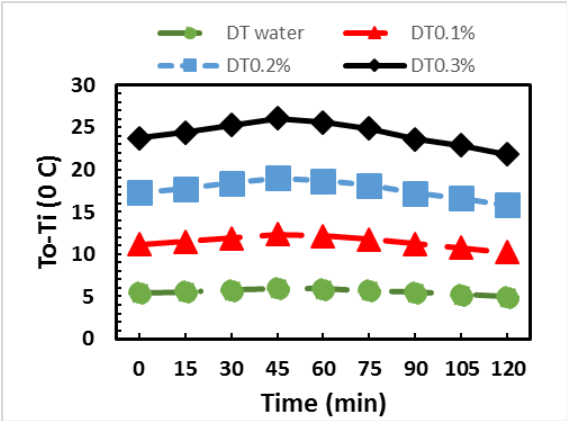

Figure 8. Investigation of inlet-outlet temperature difference with respect to solar irradiation in circular collector when utilizing various concentration of pure water and silver-water nanofluid at (Re=6004)

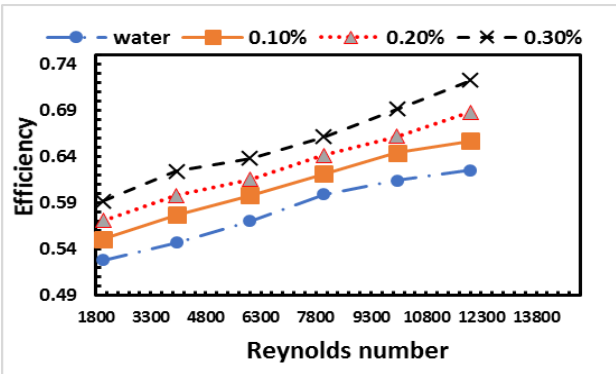

Figure 9. Efficiency of the circular collector at various Reynolds number for various concentrations of nanofluids

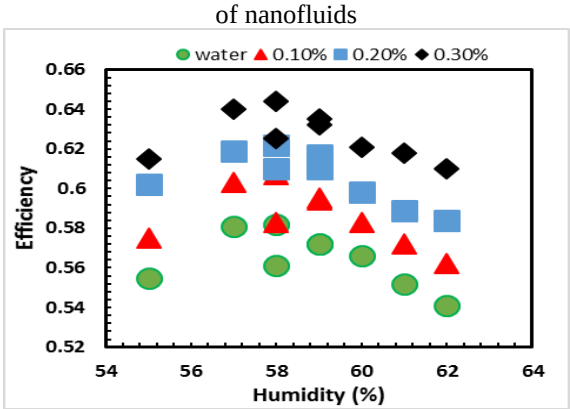

Figure 10. The effect of relative humidity on collector performance at various concentrations of nanofluid (Re=6004)

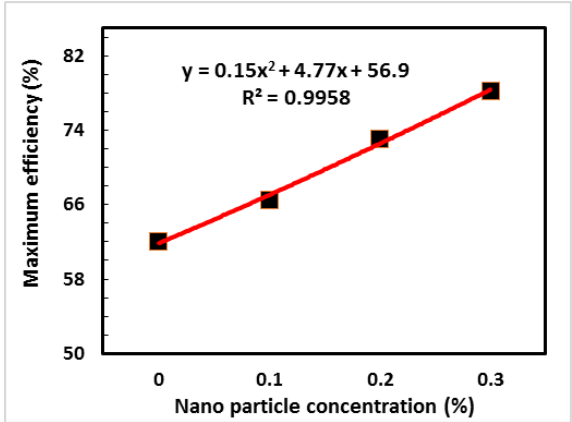

Figure 11. Maximum efficiency obtained from the effect of nanofluid concentration on circular collector performance

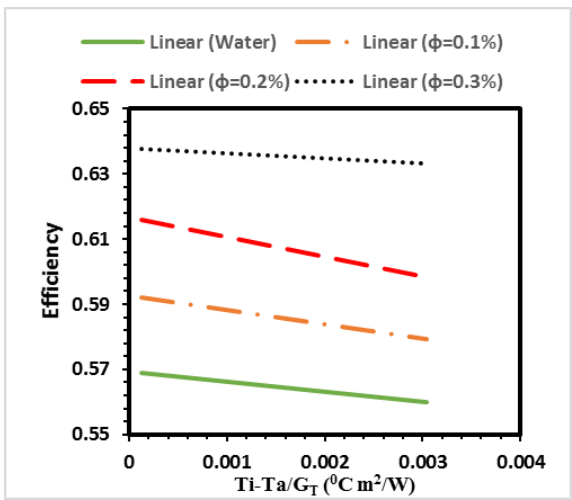

Figure 12. efficiency investigation of the collector with respect to Ti-Ta/G_T parameter in Re=6004

Table 5. Curve fitting results of using Eq. (7) for water and nanofluid in Re=6004

Coolant	$F_R(\tau\alpha)$	$F_R(U_L)$
Water	0.5693	3.1529
Nanofluid (0.1%)	0.5925	4.371
Nanofluid (0.2%)	0.6167	6.055
Nanofluid (0.3%)	0.6379	1.544

Table 6. Comparing the present study with previous research

Researcher	nanofluid	Flow rate	concentrations	Performance evaluation
Yousefi et al. [25]	Al_2O_3-water	1-3 lit/min	0.2%	28.3% up to water
Sint et al [26]	CuO-water	1.2 lit/min	0.1-3.5%	5%
Gorji & Ranjbar [27]	Ag-water	10 ml/min	>100 ppm	Optimum=51.4%
Abdelrazika et al. [28]	Ag-water	-	0.005%	7%
Gorji & Ranjbar [29]	Ag-water	20 ml/min	40ppm	11%
Zeng &Xuan [30]	Sio2/Ag-water	-	0.1%	31%
Lazarus et al. [31]	Ag-water	6 lit/min	0.04%	8% up to water
Sundar et al [32]	Al_2O_3-water	5 kg/min	0.1-0.3	18%
Present study	Ag. water	0.6gpm	0.1-0.3	14.8% up to water

4-Conclusion

The circular collector with spiral pipes that extends from the edge of the collector to its center, with ordinary water-operating fluid and silver-water nanofluid in three concentrations of 0.1%, 0.2% and 0.3% in different environmental conditions has been studied experimentally. The thermal efficiency of the helical circular collector is evaluated based on the ASHRAE standard at different flow rates and in different operating conditions. The results show that compared to pure water, nanofluid of silver-water has a better performance. Also, as the volume flow rate of both pure water and nanofluid increases, the collector efficiency increases, which is mainly due to an increase in the Reynolds number and then the Nusselt number. However, the changes are more remarkable for silver-water nanofluid in comparison with water. Additionally, the higher the nanofluid concertation, the higher the efficiency of the collector, which is mainly due to the presence of motions in nanoparticles dispersed in solution, especially Brownian motions. Also, due to the presence of spiral pipes, the increase in flow causes an increase in the production of secondary flows and therefore is of higher efficiency. The experimental results also represented that the collector efficiency becomes higher with solar irradiation increment. This increase is directly related to the nanofluid concentration, which means that the higher the nanofluid concentration, the higher the collector efficiency growth. In addition, air humidity with the concentration of nanofluids has no significant relationship in reducing or increasing efficiency. The highest efficiency obtained from this collector at a nanofluid concentration of 0.3% and a flow rate of 2.268 lpm was about 80.3%, which has increased by more than 14.8% compared to pure water.

Nomenclature

Parameter	Specification	Unit
A_C	Collector area	(m^2)
C_p	Specific heat for fluid	(J/Kg k)
$C_{p,nf}$	Specific heat for nsnofluid	(J/Kg k)
$C_{p,np}$	Specific heat for nanoparticles	(J/Kg k)
$C_{p,bf}$	Specific heat for basefluid	(J/Kg k)
F_R	Coefficient of energy in collector	-
G_T	Incident sun radiation	(W/m^2)
$\dot{m}$	Mass flow rate	(Kg/s)
Q_u	Useful energy gained from collector	(W)
S_η	Uncertainty	%
T_a	Ambient temperature	(^{0}C)
T_{in}	Inlet temperature to the collector	(^{0}C)
T_o	outlet temperature of the collector	(^{0}C)
U_L	Total loss energy coefficient	(W/m^2 K)
$T\alpha$	Absorption-transmittance product	-
φ	Nanofluid concentration	%
η_i	Instantaneous collector efficiency	%

References

1. Ouagued, M., *Magnesium–Chlorine Cycle for Hydrogen Production Driven by Solar Parabolic Trough Collectors.* Journal of Solar Energy Research, 2021. 6: p. 799-813.
2. Rezvanpour, M., Borooghani, D., Torabi, F., Pazoki, M., *Using CaCl2• 6H2O as a phase*

change material for thermo-regulation and enhancing photovoltaic panels' conversion efficiency: Experimental study and TRNSYS validation. Renewable Energy, 2020. **146**: p. 1907-21.

3. Noghrehabadi, A., Hajidavalloo, E., Moravej, M., *Experimental investigation of efficiency of square flat-plate solar collector using SiO2/water nanofluid.* Case Studies in Thermal Engineering, 2016. **8**: p. 378-86.
4. Mojtaba Moravej., *AN Experimental Study of the Performance of a Solar Flat Plate Collector with Triangular Geometry.* Journal of Solar Energy Research, 2021. **6**: p. 923-936.
5. Saffarian, M., Moravej, M., Doranehgard, M., *Heat transfer enhancement in a flat plate solar collector with different flow path shapes using nanofluid*. Renewable Energy, 2020. **146**: p. 2316-29.
6. Samiezadeh, S., Qasemian, A., Sohani, A., Rezaei, A., Khodaverdian, R., Soltani, R., et al., *Energy and environmental enhancement of power generation units by means of zero-flow coolant strategy.* International Journal of Energy Research, 2021. **45**: p. 10064-10085.
7. Sakhaei, S., Valipour, M., *Thermal performance analysis of a flat plate solar collector by utilizing helically corrugated risers: An experimental study.* Solar Energy, 2020. **207**: p. 235-46.
8. Sundar, S., Sintie, Y., Said, Z., Singh, M., Punnaiah, V., Sousa, A., *Energy, efficiency, economic impact, and heat transfer aspects of solar flat plate collector with Al2O3 nanofluids and wire coil with core rod inserts.* Sustainable Energy Technologies and Assessments, 2020. **40:** 100772.
9. Noghrehabadi, A., Hajidavalloo, E., Moravej, M., *An experimental investigation on the performance of a symmetric conical solar collector using SiO2/water nanofluid.* Transp Phenom Nano Micro Scales, 2016. **5**: p. 23-9.
10. Moravej, M., Bozorg, M., Guan, Y., Li, L., Doranehgard, M., Hong, K., et al., *Enhancing the efficiency of a symmetric flat-plate solar collector via the use of rutile TiO2-water nanofluids.* Sustainable Energy Technologies and Assessments, 2020. **40**: 100783.
11. Rajput, N., Shukla, D., Rajput, D., Sharm, S., *Performance analysis of flat plate solar collector using Al2O3/distilled water nanofluid: an experimental investigation.* Materials Today: Proceedings, 2019. **10**: p. 52-9.
12. Zayed, M., Zhao, J., Du, Y., Kabeel, A., Shalaby, S., *Factors affecting the thermal performance of the flat plate solar collector using nanofluids: A review.* Solar Energy, 2019. **182**: p. 382-96.
13. Wole-Osho, I., Okonkwo, E., Kavaz, D., Abbasoğlu, S., *Energy, Exergy, and Economic Investigation of the Effect of Nanoparticle Mixture Ratios on the Thermal Performance of Flat Plate Collectors Using Al 2 O 3–ZnO Hybrid Nanofluid.* Journal of Energy Engineering, 2021. **147**: 04020083.
14. Stalin, P., Arjunan, T., Matheswaran, M., Sadanandam, N., *Experimental and theoretical investigation on the effects of lower concentration CeO 2/water nanofluid in flat-plate solar collector.* Journal of Thermal Analysis and Calorimetry, 2019. **135**: p. 29-44.
15. Mirzaei, M., *Experimental investigation of CuO nanofluid in the thermal characteristics of a flat plate solar collector.* Environmental Progress and Sustainable Energy, 2019. **38**: p. 260-7.
16. Eidan, A., AlSahlani, A., Ahmed, A., Al-fahham, M., Jalil, M., *Improving the performance of heat pipe-evacuated tube solar collector experimentally by using Al2O3 and CuO/acetone nanofluids*. Solar Energy, 2018. **137**: p. 780-8.
17. Kiliç, F., Menlik, T., Sözen, A., *Effect of titanium dioxide/water nanofluid use on thermal performance of the flat plate solar collector.* Solar Energy, 2018. **164**: p. 101-8.
18. Okonkwo, E., Wole-Osho, I., Kavaz, D., Abid, M., Al-Ansari, T., *Thermodynamic evaluation and optimization of a flat plate collector operating with alumina and iron mono and hybrid nanofluids.* Sustainable Energy Technologies and Assessments, 2020. **37**: 100636.
19. Jiang, Y., Zhang, H., You, S., Fan, M., Wang, Y., and Wu, Z. *Dynamic performance modeling and operation strategies for a v-corrugated flat-plate solar collector with movable cover plate.* Applied Thermal Engineering, 2021. **197:** 117374.
20. Noghrehabadi, A., Hajidavalloo, E., Moravej, M., *An experimental investigation of performance of a 3-D solar conical collector at different flow rates.* Journal of Heat and Mass Transfer Research, 2016. **3**: p. 57-66.
21. Sakhaei, S. A., Valipour, M. S., *Performance enhancement analysis of the flat plate collectors: a comprehensive review*. Renewable and

Sustainable Energy Reviews, 2019. **102**: p. 186-204.
22. STANDARD, ASHRAE. 93-77, *Methods of testing to determine the thermal performance of solar collectors. American Society of Heating. Refrigeration and Air Conditioning Engineers,* Inc., NY, 1977. New York.
23. Duffie, J., Beckman, W., Blair, N., *Solar engineering of thermal processes, photovoltaics and wind*. John Wiley and Sons, 2020.
24. Holman, J. P., *Experimental methods for engineer*, Mc Grow Hill, Eight edition, 2012.
25. Yousefi, T., Veysi, F., Shojaeizadeh, E., and Zinadini, S., *An experimental investigation on the effect of Al2O3–H2O nanofluid on the efficiency of flat-plate solar collectors.* Renewable Energy, 2012. **39**: p. 293-298.
26. Sint, N. K. C., Choudhury, I. A., Masjuki, H. H., and Aoyama, H., *Theoretical analysis to determine the efficiency of a CuO-water nanofluid based-flat plate solar collector for domestic solar water heating system in Myanmar.* Solar Energy, 2017. **155**: p. 608-619.
27. Gorji, T. B., and Ranjbar, A. A., *Thermal and exergy optimization of a nanofluid-based direct absorption solar collector.* Renewable Energy, 2017. **106**: p. 274-287.
28. Abdelrazik, A. S., F. A. Al-Sulaiman, and R. Saidur., *Optical behavior of a water/silver nanofluid and their influence on the performance of a photovoltaic-thermal collector*. Solar Energy Materials and Solar Cells, 2019. **201**: p. 110054.
29. Gorji, Tahereh B., and A. A. Ranjbar., *A numerical and experimental investigation on the performance of a low-flux direct absorption solar collector (DASC) using graphite, magnetite and silver nanofluids.* Solar Energy, 2016. **135**: p. 493-505.
30. Zeng, Jia, and Yimin Xuan., *Enhanced solar thermal conversion and thermal conduction of MWCNT-SiO2/Ag binary nanofluids*. Applied Energy, 2018. **212**: p. 809-819.
31. Lazarus, G., Siddharth, R. O. Y., Kunhappan, D., Cephas, E., and Wongwises, S., *Heat transfer performance of silver/water nanofluid in a solar flat-plate collector*. Journal of Thermal Engineering, 2015. **1**: P. 104-112.
32. Sundar, L. S., Singh, M. K., Punnaiah, V., and Sousa, A. C., *Experimental investigation of Al2O3/water nanofluids on the effectiveness of solar flat-plate collectors with and without twisted tape inserts.* Renewable energy, 2018. **119**: p. 820-833.